Electric-Field-Induced Structure in Polymer Solutions near the Critical Point

Denis Wirtz, Klaus Berend, and Gerald G. Fuller*

Department of Chemical Engineering, Stanford University, Stanford, California 94305-5025

Received July 13, 1992; Revised Manuscript Received September 29, 1992

ABSTRACT: In the vicinity of the coexistence curve, binary solutions exhibit large concentration fluctuations. Such fluctuations can be anisotropically distorted through the application of an electric field, which induces both electric birefringence and enhanced forward light scattering as the system approaches the coexistence curve. Using time-dependent small-angle light scattering (SALS) and form dichroism measurements on semidilute polystyrene/cyclohexane systems (molecular weight range 400 000–1 800 000), two new phenomena have been observed: electric scattering dichroism in the one-phase region and electric-field-induced remixing in the two-phase region. A mean-field theory that predicts the evolution of the scattering patterns in the presence of an electric field above the coexistence curve has been developed. In particular, it is predicted that, in the plane perpendicular to the propagation of the incident light, circular scattering patterns become elliptical patterns having the minor axis along the direction of the applied field. As a consequence, scattering dichroism is shown to be induced in the vicinity of the critical point. Moreover, the same phenomenological model predicts that the presence of an electric field lowers the coexistence curve and results in electric-field-induced remixing of binary mixtures at a temperature below the quiescent coexistence curve. The influence of temperature, molecular weight, and concentration of the polymer in solution as well as the influence of the electric field strength on SALS patterns and induced scattering dichroism measurements is studied. The experimental observations are in fairly good agreement with the trends predicted by a phenomenologically-based, mean-field theory.

1. Introduction

The study of the phase behavior of polymer/solvent systems started in 1942 with the seminal work of Flory.[1] He found that in the poor solvent region, between the Θ-temperature and the quiescent coexistence curve, both repulsive and attractive forces between monomers are present. In addition, at the Θ-temperature the attractive and the repulsive effects compensate exactly. When lowering the temperature of a polymer solution with a concentration close to the critical concentration (corresponding to the top of the coexistence curve), the length scale of the concentration fluctuations increases and reflects the fact that polymer–polymer and solvent–solvent interactions dominate polymer–solvent interactions. Eventually, this results in the transparent polymer solution becoming turbid. Associated with the critical point is the phenomenon of critical opalescence studied in detail by Debye and co-workers,[2] which is an effect of enhanced forward scattering when approaching the critical point. Further lowering the temperature below the coexistence curve causes the solution to demix into two phases with the compositions given by Maxwell's rule.

Critical fluctuations can be deformed by an external field, such as a magnetic field (Cotton–Mouton effect[3]), a flow field,[4] or an acoustic wave.[5] In 1964, Debye and Kleboth[6] studied the effect of an electric field on the critical opalescence of low-molecular-weight solutions (nitrobenzene/2,2,4-trimethylpentane). They observed an increase in the transmitted intensity in the presence of an electric field. They modeled their findings by adding an electric contribution to the free energy of the binary mixture, which resulted in a negative shift of the critical temperature. In 1980, Pyzuk[7] published electrooptical Kerr effect measurements (electric birefringence) for mixtures of propionitrile/hydrocarbons in the critical region. In 1985, Degiorgio and co-workers[8] measured transient electric birefringence for critical nonionic micellar solutions and, in subsequent works,[9] showed that, when the electric field is turned off, relaxation of the concentration fluctuations is not exponential but instead follows a stretched exponential law.

It is the goal of this paper to present experimental results along with phenomenological models of the effects of an electric field on the structure of the concentration fluctuations in semidilute polymer solutions. Presented here are the first scattering dichroism measurements induced by an electric field near the critical point of nonpolar, nonabsorbing polymer solutions. Simultaneously, small-angle light scattering (SALS) measurements of the structure factor were performed. From these results, both birefringence and dichroism were computed and compared against direct measurements of these anisotropies. SALS measurements also showed, for the first time, a phenomenon of electric-field-induced remixing for polymer solutions and low-molecular-weight solutions at a temperature below the coexistence curve.

2. Theory

This section outlines the conditions for which scattering dichroism can be induced by an electric field applied to a polymer solution near its critical point. The dynamics of the concentration fluctuations in an electric field can be described by a Langevin equation that includes a contribution from three forces: a thermodynamic force due to osmotic pressure and inhomogeneities in the concentration, a dipolar force due to interactions between concentration fluctuations, and a random force due to Brownian collisions between monomers. In addition, a simple thermodynamic approach is used to demonstrate the mechanism by which a stationary electric field can lower both the coexistence and the spinodal curves of a polymer/solvent system and the manner by which an electric field decreases the osmotic pressure. Finally, the influence of parameters such as concentration, molecular weight, field strength, and temperature on electric-field-induced remixing is analyzed for a polymer solution at a temperature below the coexistence curve.

2.1. Structure Factor. Fluctuations in the local permittivity tensor, ϵ, may arise from spatial and temporal fluctuations in the density, temperature, and concentration of a solution. This paper only considers concentration

0024-9297/92/2225-7234$03.00/0

fluctuations at constant temperature and constant volume. Moreover, the fluctuating part of the dielectric tensor $\delta\epsilon$ is assumed to be isotropic and linear in the order parameter $\delta c(\mathbf{r},t)$

$$\delta\epsilon_{ij}(\mathbf{r},t) = (\partial\epsilon/\partial c)\,\delta c(\mathbf{r},t)\,\delta_{ij} \tag{1}$$

The dielectric tensor can be written as

$$\epsilon_{ij}(\mathbf{r},t) = \epsilon\delta_{ij} + \delta\epsilon_{ij}(\mathbf{r},t) \tag{2}$$

where ϵ is the uniform dielectric constant of the sample. Fluctuations in ϵ_{ij} induce dipole fluctuations, which cause the electric field to vary about the mean field $\langle\mathbf{E}\rangle$:

$$E_i = \langle E_i\rangle + \delta E_i \tag{3}$$

where $\delta\mathbf{E}$ is the electric field of the light scattered from a concentration fluctuation. The classical expression for the scattering intensity, I, using the far-field approximation, is given by[10]

$$I(\mathbf{q},r) = \frac{I_0}{(4\pi r)^2}|\mathbf{k}_s \times \mathbf{k}_s \times \mathbf{n}_i|^2 V\left(\frac{\partial\epsilon}{\partial c}\right)^2 \int d\mathbf{r}' \exp(-i\mathbf{q}\mathbf{r}') \times \langle\delta c(\mathbf{r}',t)\,\delta c(\mathbf{0},t)\rangle \tag{4}$$

Here r is the distance between the scattering fluctuation and the detector; I_0 is the intensity of the probing light; V is the system volume; $\mathbf{n}_i$ is the vector describing the polarization state of the incident light; and $\mathbf{q} = \mathbf{k}_s - \mathbf{k}_i$ is the scattering vector defined as the difference between the wave vector of the scattered light, $\mathbf{k}_s$, and the wave vector of the incident light, $\mathbf{k}_i$, having a wavelength λ_i and parallel to $\mathbf{n}_i$. If $|\mathbf{k}_s| \cong |\mathbf{k}_i| \cong 2\pi/\lambda_i$ and the Bragg condition applies, then

$$q = |\mathbf{q}| = \frac{4\pi}{\lambda_i}\sin\left(\frac{\theta}{2}\right) \tag{5}$$

where θ is the scattering angle between $\mathbf{k}_s$ and $\mathbf{k}_i$.

The structure factor is defined as the Fourier transform of the equal-time spatial correlation function:

$$S(\mathbf{q}) = \int d\mathbf{r}' \exp(-i\mathbf{q}\mathbf{r}')\langle\delta c(\mathbf{r}',t)\,\delta c(\mathbf{0},t)\rangle \tag{6}$$

Since the scattering intensity is proportional to the structure factor in view of eqs 4 and 6, measurements of the scattering intensity at various scattering angles allow direct estimates of the external field-induced anisotropy in the structure factor. At equilibrium, in the absence of an electric field, critical scattering fluctuations scatter light isotropically. The structure factor is thus isotropic and can be approximated by the Orstein–Zernike Lorentzian for small scattering angles[11]

$$S_o(\mathbf{q}) = \frac{1}{\xi^{-2} + q^2} \tag{7}$$

The equilibrium correlation length ξ follows a power law behavior near criticality, $\xi = \xi_0(T/T_c - 1)^{-\nu}$, where the theoretical value of the critical exponent ν is 0.630[11] and ξ_0 is a nonuniversal amplitude which is on the order of a few angstroms for a polymer/solvent system such as polystyrene/cyclohexane.[12] The growth of concentration fluctuations near criticality reflects the existence of long-range interactions between monomers in the vicinity of the critical point. According to eq 7, when no field is applied, scattering patterns are concentric circles in the plane perpendicular to the propagation of the incident light.

Before presenting the dynamical equations for the concentration fluctuations in the presence of an electric field, $\mathbf{E}$, a simple derivation of the steady-state structure factor is given. In the mean-field approximation, the free energy is given by the Landau–Ginsburg[13] truncated Taylor series in the concentration deviation, $\delta c(\mathbf{r})$

$$\Delta\mathcal{F} = \frac{1}{2}\int_V d\mathbf{r}\,[C_1(\delta c)^2 + C_2|\nabla\delta c|^2 + C_3|\mathbf{E}\delta c|^2 + C_4(\mathbf{E}\cdot\nabla\delta c)^2] \tag{8}$$

Terms linear in $\delta c(\mathbf{r})$ have been eliminated since concentration fluctuations must increase the free energy and $\delta c(\mathbf{r})$ has no definite sign. Terms linear in the gradient of the fluctuation are also eliminated because of the translational invariance of the system. For simplicity, non-Gaussian corrections have been neglected; these are proportional to $(\delta c)^4$ and are responsible for deviations in the critical exponents from their mean-field values in the region close to the critical temperature. Notice that $\Delta\mathcal{F}$ is expressed in thermal units $k_BT = \beta$, as are all energies in the remainder of the paper. $\Delta\mathcal{F}$ can be expressed in terms of the Fourier components of the concentration fluctuation, $\delta c(\mathbf{q})$

$$\Delta\mathcal{F} = \frac{1}{2}\sum_{\mathbf{q}}(C_1 + C_2q^2 + C_3E^2 + C_4E^2q_x^2)|\delta c(\mathbf{q})|^2 \tag{9}$$

assuming that $\mathbf{E} = E\mathbf{n}_x$. The Gaussian probability distribution associated with each fluctuation is proportional to a Boltzmann factor $\exp[-\Delta\mathcal{F}]$:

$$P_{\mathbf{q}} \sim \exp[-(C_1 + C_2q^2 + C_3E^2 + C_4E^2q_x^2)|\delta c(\mathbf{q})|^2] \tag{10}$$

and, therefore, the structure factor is

$$S(\mathbf{q},\mathbf{E}) = \overline{|\delta c(\mathbf{q})|^2} = \frac{1}{(C_1 + C_2q^2 + C_3E^2 + C_4E^2q_x^2)} \tag{11}$$

Now in a different and perhaps more physical approach, a phenomenological model is presented allowing us to differentiate the relevant forces acting on both the solvent molecules and the polymer chains. This model considers the dynamics of deformation of the concentration fluctuations in a steady electric field. It is used here primarily to explain the formation of steady-state structures and will be used, in a subsequent paper, to describe the critical dynamics of relaxation of fluctuations at the inception and the cessation of an electric field. It is based on the two-fluid model first introduced by Jannink and de Gennes[14] and used subsequently by several authors[15-18] to study flow-induced enhancement of critical fluctuations and critical dynamics of gels. Let $\mathbf{v}$ be an average velocity $\mathbf{v} = \varphi\mathbf{v}_p + (1-\varphi)\mathbf{v}_s$, where φ is the polymer volume fraction and $\mathbf{v}_p$ and $\mathbf{v}_s$ are the velocities of the polymer "fluid" and the solvent, respectively. With the condition of incompressibility, $\nabla\cdot\mathbf{v} = 0$, the following equations of continuity for the polymer and the solvent can be derived

$$\partial\varphi/\partial t + \nabla\cdot(\mathbf{v}_p\varphi) = 0 \tag{12}$$

$$\frac{\partial}{\partial t}(1-\varphi) + \nabla\cdot[(1-\varphi)\mathbf{v}_s] = 0 \tag{13}$$

The stress acting on a volume element of a semidilute polymer solution in an electric field includes three terms. The first term is the osmotic pressure $\pi_{ij} = -\pi(\varphi)\,\delta_{ij}$ which depends on the polymer concentration. The second contribution to the stress is the drag force due to the relative motion of the polymer and solvent. The latter is proportional to the Darcy coefficient, λ, in the two-fluid model. For a semidilute polymer solution in a poor solvent, $\lambda(\varphi) \sim \eta_s\xi^2(\varphi)$ where η_s is the solvent shear viscosity and

$\xi(\varphi)$ the concentration-dependent correlation length (in Θ solvents $\lambda \sim \eta_s\varphi^2$). Last, in the presence of an electric field, there is a dipolar interaction tensor, $\Pi^{(E)}$, that will be specified below.

A balance of the forces acting on a small volume of polymer solution gives rise to Euler equations for the polymer momentum density, $\mathbf{g}_p = \varphi\rho_p{}^0\mathbf{v}_p$, and the solvent momentum density, $\mathbf{g}_s = (1-\varphi)\rho_s{}^0\mathbf{v}_s$. Here, $\varphi\rho_p{}^0$ is the mass of polymer and $(1-\varphi)\rho_s{}^0$ is the mass of solvent in the solution. The Euler equations are

$$\partial\mathbf{g}_p/\partial t = \nabla\cdot\Pi^{(o)} + \nabla\cdot\Pi^{(E)} + \lambda(\mathbf{v}_s - \mathbf{v}_p) \tag{14}$$

$$\partial g_s/\partial t = -\lambda(\mathbf{v}_s - \mathbf{v}_p) \tag{15}$$

where $\nabla\cdot\Pi^{(o)}$ is the thermodynamic force density resulting from osmotic pressure and concentration fluctuations and $\nabla\cdot\Pi^{(E)}$ is the dipolar force between concentration fluctuations in the presence of an electric field. Note that these equations do not include elastic and viscous stresses, which are second order in the concentration fluctuation in the absence of a flow field. The acceleration equation (eq 14) for the polymer fluid includes the polymer osmotic pressure, the relative drag force, and the dipole–dipole interaction forces between polymer monomers. The equation of motion (eq 15) for the solvent momentum includes only the drag force. Inertial terms in the polymer momentum equation can be neglected since $\varphi\rho_p{}^0 \ll (1-\varphi)\rho_s{}^0$, and, therefore, the relative velocity field between the solvent and the polymer fluid is reduced to

$$\mathbf{v}_p - \mathbf{v}_s = \frac{1}{\lambda}\nabla\cdot\Pi \tag{16}$$

where $\nabla\cdot\Pi = \nabla\cdot\Pi^{(o)} + \nabla\cdot\Pi^{(E)}$ is the total force density. Substituting eq 16 into eq 15 and using eqs 12 and 13, a kinetic equation for the polymer volume fraction can be derived as

$$\frac{\partial\varphi}{\partial t} + \mathbf{v}\cdot\nabla\varphi \cong \Theta_\varphi - \nabla\cdot\left[\frac{1}{\zeta(\varphi)}\nabla\cdot\Pi\right] \tag{17}$$

where $\zeta(\varphi) = \lambda(\varphi)/\varphi$ is the friction coefficient of the polymer/solvent system and Θ_φ is white Gaussian noise that is related to ζ through the fluctuation–dissipation theorem.[19] It is a random force that takes account of the collisions between the monomers in solution. In equation 17, it is assumed that $\varphi \ll 1$. The osmotic pressure is related to the Flory–Huggins free energy of mixing, $f(\varphi,T)$, by $\pi(\varphi) = \varphi\,\partial f/\partial\varphi - f$, where $f = (\varphi/N)\ln\varphi + (1/2-\chi)\varphi^2 + \varphi^3/6 + O(\varphi^4)$[20] for small polymer volume fractions (χ is the Flory–Huggins interaction parameter and N is the number of segments per polymer chain). Hence, $\pi(\varphi) \cong (1/2-\chi)\varphi^2$ for $1/N \ll \varphi \ll 1$. If one introduces the Helmholtz free energy $\mathcal{F}$ as the sum of the thermodynamic free energy due to concentration fluctuations[18] and the free energy due to the presence of an electric field

$$\mathcal{F} = \int_V d\mathbf{r}\left[f(\varphi,T) + \frac{1}{2}K_1|\nabla\varphi|^2 + \frac{1}{2}K_2|\mathbf{E}\varphi|^2 + \frac{1}{2}K_3(\mathbf{E}\cdot\nabla\varphi)^2\right] \tag{18}$$

then the total force density acting on polymer segments is given by[17]

$$\mathbf{F} = \mathbf{F}^{(o)} + \mathbf{F}^{(E)} = \nabla\cdot\Pi = -\varphi\nabla(\delta\mathcal{F}/\delta\varphi) \tag{19}$$

Here, K_2 and K_3 are two-body interaction parameters defining the strengths of the electric binary interactions between concentration fluctuations and between their gradients. The second term in eq 18 represents the increase of the free energy due to inhomogeneities in the polymer volume fraction. In the mean-field approximation, the equilibrium correlation length in the absence of an external field is $\xi = [(1-2\chi)/K_1]^{-0.5}$.[13] One can rewrite eq 17 using eq 19

$$\frac{\partial\varphi}{\partial t} + \mathbf{v}\cdot\nabla\varphi - \nabla\cdot\left[\frac{1}{\zeta}\varphi\nabla\left(\frac{\delta\mathcal{F}}{\delta\varphi}\right)\right] = \Theta_\varphi \tag{20}$$

The total stress tensor Π is[18]

$$\Pi = \pi(\varphi)\,\delta - \left[\frac{1}{2}K_1|\nabla\varphi|^2 + K_1\varphi\nabla^2\varphi\right]\delta + K_1(\nabla\varphi\nabla\varphi) + \frac{1}{2}K_2|\mathbf{E}\varphi|^2 + \frac{1}{2}K_3(\mathbf{E}\nabla\varphi)^2 - K_3(\mathbf{E}\varphi\mathbf{E}\nabla^2\varphi) \tag{21}$$

where δ is the unit tensor. From this last equation and eq 19, the total force can be computed as

$$\mathbf{F} = \nabla\pi - \varphi\nabla\cdot[(K_1\nabla^2\varphi - K_2E^2\varphi)\delta + K_3(\mathbf{E}\nabla^2\varphi\mathbf{E})] = \varphi\nabla\cdot[(f'' + K_2E^2 - K_1\nabla^2)\varphi\delta - K_3(\mathbf{E}\nabla^2\varphi\mathbf{E})] \tag{22}$$

where $f'' \cong (1-2\chi)$ for semidilute polymer/solvent systems. First-order perturbation of the volume fraction as $\varphi(\mathbf{r},t) = \varphi_o + \delta\varphi(\mathbf{r},t)$ (φ_o is the overall volume fraction of the polymer solution) and of the velocity field $\mathbf{v} = \langle\mathbf{v}\rangle + \delta\mathbf{v}(\mathbf{r},t)$, and substitution into eq 22 yield, upon Fourier transformation, a Langevin equation for the Fourier components of the concentration fluctuation $\delta\varphi(\mathbf{q})$

$$\frac{\partial}{\partial t}\delta\varphi(\mathbf{q},t) = -\lambda_o q^2[(1-2\chi+K_2E^2) + K_1q^2 + K_3q_x{}^2E^2]\delta\varphi(\mathbf{q},t) + \Theta_q \tag{23}$$

where $\lambda_o = \varphi_o/\zeta$. In writing eq 23, we have introduced a Cartesian set of coordinates in the $\mathbf{q}$-space: q_z, in the direction $-\mathbf{k}_i$; q_x, in the direction $\phi = 0$, parallel to the electric field; and q_y in the direction $\phi = \pi/2$, perpendicular to the field (ϕ is the azimuthal angle in the plane perpendicular to the incident light). The convection term present in eq 20 becomes $\mathbf{v}\nabla\varphi = \delta\mathbf{v}\nabla\delta\varphi$ in the absence of a flow field and has been neglected in eq 23, which has been written to first order in fluctuations. An equation similar to eq 23 can be written for $\delta\varphi^*(\mathbf{q}) = \delta\varphi(-\mathbf{q})$; thus, the diffusion equation for the structure factor, $S(\mathbf{q},\mathbf{E},t) = \langle\delta\varphi(\mathbf{q},t)\,\delta\varphi(-\mathbf{q},t)\rangle$, is

$$\frac{\partial}{\partial t}S(\mathbf{q},\mathbf{E},t) = -2\lambda_o q^2[(1-2\chi+K_2E^2) + K_1q^2 + K_3q_x{}^2E^2]S(\mathbf{q},\mathbf{E},t) + \langle\Theta(\mathbf{q},t)\,\Theta(-\mathbf{q},t)\rangle \tag{24}$$

where $\langle\Theta(\mathbf{q},t)\,\Theta(-\mathbf{q},t)\rangle = 2\lambda_o q^2\delta(t-t')$. From this dynamical equation, relaxation times of the concentration fluctuations upon inception and cessation of the orientational electric field, $\tau_q \sim S(\mathbf{q},\mathbf{E})/\lambda_o q^2$, can be calculated. It can be readily seen that approaching the critical point causes the well-known critical slowing down of the fluctuations. Moreover, as expected, fluctuation modes at large q values relax faster than those at small q. Note that very near the critical point, the decay rate of order-parameter fluctuations becomes independent of temperature and depends only on q.

At steady state, one recovers the same structure factor as eq 11

$$S(\mathbf{q},\mathbf{E}) = \frac{1}{\kappa(E) + K_1q^2 + K_3E^2q_x{}^2} \tag{25}$$

where $\kappa(E) = \kappa + K_2E^2 = 1 - 2\chi + K_2E^2$. Equation 25 can be rearranged as follows:

$$1/S(\mathbf{q},\mathbf{E}) = \kappa(E)[1 + \xi_E{}^2q_y{}^2 + \xi_E{}^2q_x{}^2(1 + E^2K_3/K_1)] \tag{26}$$

In the last equation, a "transverse" correlation length ξ_E

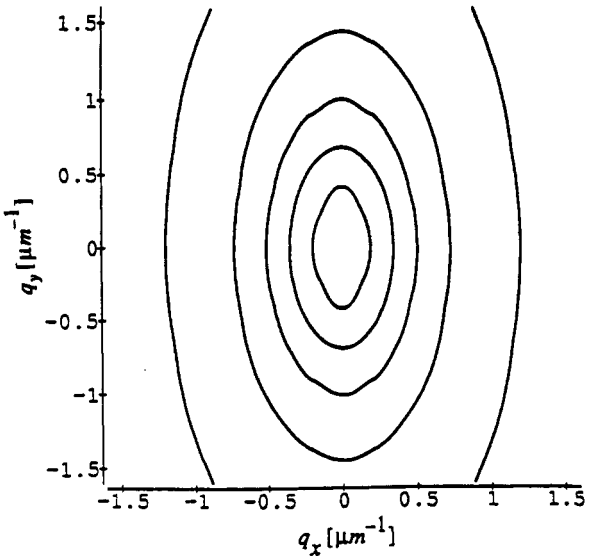

Figure 1. Contour plots of the structure factor in the presence of an electric field as ellipses in the $q_x - q_y$ plane. The length of the major axis is only slightly increased as an electric field is applied. The length of the minor axis, parallel to the field, depends on both $T - T_c$ and the strength of the field.

has been introduced, which is given by

$$\xi_E = (\kappa(E)/K_1)^{-0.5} = \xi_0[(T - T_c(E))/T_c]^{-0.5} \quad (27)$$

$$\xi_0 = (K_1 T_c/A)^{-0.5} \quad (28)$$

since $\kappa = A(T - T_c)$[13] (A = constant). Therefore, one effect of the electric field on a binary liquid mixture is to shift the critical temperature from T_c to $T_c(E) = T_c - K_2E^2/A$. This effect will be considered in more detail in section 2.3. As a consequence, at a fixed temperature the average size of the critical concentration fluctuations is slightly decreased from ξ to ξ_E in the direction perpendicular to the field and increased from ξ to $\xi_E(1 + K_3E^2/K_1) \simeq \xi(1 + K_3E^2/K_1)$ in the direction parallel to the field.

Note that if dipole–dipole interactions between monomers were dominant, the structure factor would be[21]

$$S(\mathbf{q},\mathbf{E}) = \frac{1}{(1 - 2\chi) + K_1q^2 + g_E(q_x/q)^2} \quad (29)$$

where $g_E \sim E^2$. Contour plots of this structure factor are "butterfly" patterns oriented in the direction perpendicular to the field. Onuki and Doi[22] used the analogy between dipolar interactions in a system of uniaxial ferromagnets (in three dimensions) and dipolar interactions between monomers to derive a similar structure factor. However, SALS experiments show that measured structure factors are not consistent with this assumption.

Both approaches (the modified Landau–Ginsburg model and the two-fluid model) show that the steady-state structure factor can be reduced to the following form:

$$\frac{1}{S(\mathbf{q},\mathbf{E})} = \kappa(E) + \left(\frac{q_x}{q_{min}}\right)^2 + \left(\frac{q_y}{q_{maj}}\right)^2 \quad (30)$$

Contour plots of the structure factor are elliptical patterns in the $q_x - q_y$ plane (see Figure 1). The minor axis is along the direction of the field. To calculate an average length of both the minor axis and the major axis from the experimental SALS data, we define the two following characteristic values of the scattering vector, q_{min} and q_{maj}, in the directions parallel and perpendicular to the field:

$$q_{maj,min}^{\ 2} = \frac{\int d\mathbf{q}\, |\mathbf{q}|^2 \Delta S(\mathbf{q},t)\, \delta(\chi_s - \varphi(\mathbf{q}))}{\int d\mathbf{q}\, \Delta S(\mathbf{q},t)\, \delta(\chi_s - \varphi(\mathbf{q}))} \quad (31)$$

where $\Delta S(\mathbf{q},t) = S(\mathbf{q},\mathbf{E},t) - S_0(q)$. The two scattering angles corresponding to the major and minor axes are $\chi_{maj} = 90°$ and $\chi_{min} = 0°$, respectively. For the major axis q_{maj} is a constant and is given by $1/q_{maj}^2 = K_1$. However, $1/q_{min}^2$ increases quadratically with the electric field, $1/q_{min}^2 = (K_1 + K_3E^2)$, for field strengths in the linear regime. From this, it can be predicted that the application of an electric field affects the shape of the initially circular patterns by reducing the length of only the minor axis along the direction of the field.

2.2. Scattering Dichroism. Recently, Doi and Onuki extended their theory of flow birefringence and dichroism[23] to electric birefringence and dichroism in critical binary systems.[22] They derived a formula relating the anisotropy of the structure factor and its moments to the anisotropy of the refractive index tensor. In general, the imaginary component of the refractive index tensor can be separated into an intrinsic part and a form part. The intrinsic contribution exists only if the molecules of the mixture absorb light anisotropically. The form contribution is due to the anisotropic scattering of light from concentration fluctuations in the presence of a distorting field. Since polymer solutions such as polystyrene/cyclohexane (PS/CH) do not absorb visible light, measurements of scattering dichroism seem to be best suited to study the dynamics of concentration fluctuations in polymer solutions near criticality. Conversely, birefringence measurements (the real part of the difference of the principal values of the refractive index tensor) are affected by both form and intrinsic effects for visible light and, therefore, cannot uniquely define orientation dynamics of polymer systems near the critical point.

In a small-angle light scattering experiment, one measures the scattering intensity for angles small enough that the scattering vector essentially lies in the plane perpendicular to the incident light ($q_x - q_y$ plane). One assumes that this region is sufficiently large to measure the nonzero part of the structure factor, the magnitude of which decreases rapidly with increasing scattering angle for large scattering fluctuations. Therefore, the refractive index tensor has unequal components only in the x–y plane. In this case, the difference in the principal values of the imaginary part of the refractive index tensor (scattering dichroism) is

$$\Delta n'' \cong \frac{\Delta\epsilon''}{2n} = \frac{\epsilon''_{xx} - \epsilon''_{yy}}{2n} \quad (32)$$

where ϵ'' is the imaginary part of the dielectric tensor and $n = \sqrt{\epsilon}$ is the uniform refractive index of the mixture. In eq 32, the anisotropic part of the dielectric tensor was assumed to be much smaller than the isotropic part. The scattering dichroism can be related to the anisotropy in the structure factor $S(\mathbf{q},\mathbf{E})$ through an integral equation[23]

$$\Delta n'' = \frac{k^3}{32\pi^2\epsilon^{3/2}}\left(\frac{\partial\epsilon}{\partial c}\right)^2 \mathrm{Im} \int d\mathbf{q}\, \frac{q_y^{\ 2} - q_x^{\ 2}}{q^2 - k^2 - i0} cS(\mathbf{q},\mathbf{E}) \quad (33)$$

In order to compute $\Delta n''$ from SALS data, eq 33 is expressed in spherical coordinates as

$$\Delta n'' = C_0 \int_0^{\pi} d\theta \sin\theta \int_0^{2\pi} d\varphi \sin\theta^2 \cos 2\varphi \, cS(\mathbf{q},\mathbf{E}) \quad (34)$$

$$C_0 = \frac{k^3}{32\pi^2\epsilon^{3/2}}(\partial\epsilon/\partial c)^2 \quad (35)$$

The constant C_0 can be estimated by turbidity measurements.

For low fields, $S(\mathbf{q},\mathbf{E})$ can be written as a linear perturbation of the Orstein–Zernike structure factor:

$$S(\mathbf{q},\mathbf{E}) = S_0(q) - K_3 S_1(q)\, q_i q_j E_i E_j \quad (36)$$

where $S_0(q)$ is given by eq 7 (where ξ is replaced by ξ_E) and $S_1(q) = S_0^2(q)$. Substituting eq 36 into eq 33, the induced dichroism can be computed from the expression of the imaginary part of the form dielectric tensor ϵ:[23]

$$\epsilon'' = \frac{K_3 C_0(\mathbf{EE})}{k^3}\int_0^{\infty} dq\, q^4 \Psi(q/2k) S_1(q) \quad (37)$$

where $\Psi(x) = \pi x^4(1-x^2)^2(1-x)$. The resulting dichroism is given by

$$\Delta n'' = BE^2 N''(k\xi) = \left(32\frac{\pi}{k}K_3 C_0 \xi\right)E^2 \int_0^1 dx\, x^5 \times (1-x)(1-x^2)^2 \frac{(k\xi)^3}{(1+4[k\xi]^2 x^2)^2} \quad (38)$$

This equation predicts that, for low fields, the dichroism follows a quadratic law in the electric field similar to the Kerr law for the electric-field-induced birefringence[7] as foreseen by Onuki and Doi.[22] The function $N''(k\xi)$ is shown in Figure 2. This figure shows that in the critical region ($k\xi \gg 1$) steady-state, induced dichroism increases with the temperature difference $T - T_c$ (at a fixed value of the wave vector of the incident light) and reaches a maximum further away from T_c ($k\xi \sim 1$), independent of the strength of the electric field to rapidly vanish in the hydrodynamic region ($k\xi \ll 1$). As an example, the maximum of $N''(k\xi)$ occurs at about $k\xi \cong 1.70$, which corresponds to a temperature distance from the critical point of $T - T_c \cong 0.048$ °C for a polystyrene/cyclohexane solution at a critical concentration (M_w = 400 000).[12]

2.3. Electric-Field-Induced Remixing. Since the pioneering research of the Debye and Kleboth,[6] little work has been done from either experimental or theoretical points of view to more thoroughly understand the thermodynamic effects of an electric field on critical concentration fluctuations in a binary mixture. They observed that above the critical point an electric field decreases the apparent absorption coefficient α, defined as $\alpha = (1/d)\ln(I_0/I_t)$, where d is the thickness of the scattering medium and I_t is the transmitted intensity. The effect was attributed to electric-field-induced lowering of the critical temperature of the mixture. In this section, Debye and Kleboth's ideas are extended to polymer/solvent systems in both the one-phase and two-phase regions. The equilibrium of a high polymer in a poor solvent between the Flory Θ-point and the coexistence curve is best described mathematically by the sum of a local two-body interaction of arbitrary sign and a local positive, e.g., repulsive, three-body interaction.[24] In that region, coils are more compact than ideal chains because of the tendency toward segregation.[20] At the Θ-temperature, the two-body interaction between monomers disappears, and only the three-body interaction subsists; the chains are nearly Gaussian. Below the coexistence curve, the polymer solution separates into a dilute phase of isolated polymer chains and a semidilute phase of strongly entangled chains.

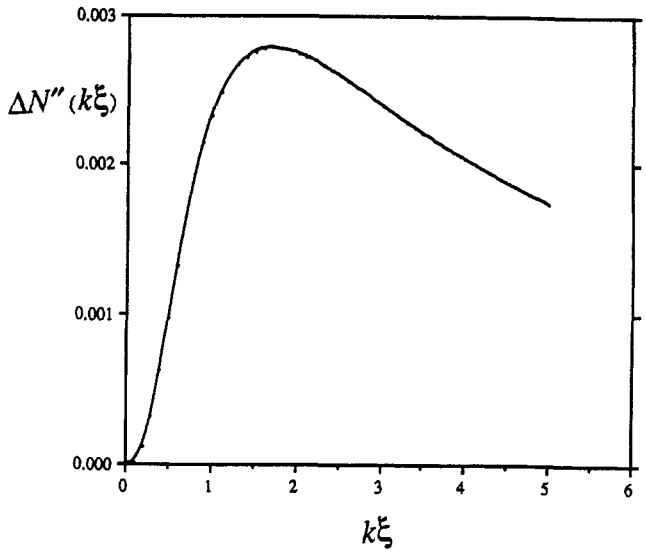

Figure 2. Scaling function $N''(k\xi)$ as a function of $k\xi$ calculated from eq 39 using the decomposition of the structure factor at low fields. k is the fixed wave vector of the probing light, and ξ is the correlation length. This graph shows that induced dichroism increases with $T - T_c$ ($\xi \sim (T - T_c)^{-0.5}$) in the critical region ($k\xi \gg 1$) before decreasing in the hydrodynamic region ($k\xi \ll 1$).

The effect of a shear flow on a semidilute polymer solution is to induce an apparent change of phase (above the coexistence curve) that is accompanied by a large increase in the turbidity at temperatures much higher than the coexistence curve.[4] In this section, the effect of an electric field is shown to induce remixing in a two-phase polymer solution at temperatures below the coexistence curve. Starting from the expression of the free energy for solutions of low polymer concentrations, within the framework of the standard continuous model[24] (simple-tree approximation), one can add a potential term due to the electric field[25]

$$\frac{\mathcal{F}}{V} = \frac{bS^2C^2}{2} + \frac{cS^3C^3}{6} + C\ln(C\nu_r) + C\mu_0 + \frac{E^2}{2\beta}(\epsilon - \epsilon_s(1 - C\nu_r N) - \epsilon_p C\nu_r N) \quad (39)$$

In eq 39 the same notation as in ref 24 has been used to facilitate the comparison with the quiescent case. Moreover, contributions due to the inhomogeneities of the polymer concentration have been disregarded because these terms are irrelevant in the present discussion. $\mathcal{F}/V$ is the excess free energy of the solution in the presence of the electric field per unit volume. The first two terms in eq 39 correspond to the energy associated with the polymer solution and include both two-body interactions of variable strength, b, and three-body interactions of constant intensity, c. The third and fourth terms are the excess entropy of mixing, where μ_0 is a constant and C is the number of polymers per unit volume. $NC\nu_r = \varphi$ is the volume fraction of polymer in solution where ν_r has the dimensions of a volume and corresponds to the volume of a site in the simple lattice model. S is the area associated with each polymer chain defined by $R^2 = \langle(\mathbf{R}(S) - \mathbf{R}(o))^2\rangle = Sd$ (d = dimension of space). If the chains are made of N links, $S = Nl^2$, where l is a characteristic length of the link.[24]

The last term in eq 39 is the excess free energy due to the field $\mathbf{E}$ and is proportional to the "excess" electric energy of the mixture which is defined as the difference between the electric energy of the mixture and the weighted average of the electric energies of the pure solvent and the

pure polymer[25]

$$\beta\Delta\mathcal{F}_E = \frac{1}{2}\mathbf{D}\cdot\mathbf{E} - \frac{1}{2}\sum_{i=s,p}\varphi_i(\mathbf{D}\cdot\mathbf{E})_i = \frac{1}{2}\epsilon E^2 - \frac{1}{2}[\varphi\epsilon_p E^2 + (1-\varphi)\epsilon_s E^2] \quad (40)$$

where ϵ is the dielectric constant of the binary mixture, ϵ_s and ϵ_p are the dielectric constants of the pure solvent and the pure polymer, respectively, and $\mathbf{D}$ is the displacement vector associated with the applied field.

Note that the correspondence between the two-body parameter b and the three-body parameter c of the continuous model and the interaction parameters χ and ν_r of the lattice model is[24]

$$bS^2 = N^2(1-2\chi)\nu_r \quad (41)$$

$$cS^3 = N^3\nu_r^2 \quad (42)$$

The osmotic pressure, π, and the chemical potential, μ, of the polymer in solution are derived from the expression of $\mathcal{F}/V$:

$$\pi = C\frac{\partial}{\partial C}\left(\frac{\mathcal{F}}{V}\right) - \left(\frac{\mathcal{F}}{V}\right) \quad (43)$$

$$\mu = \frac{\partial}{\partial C}\left(\frac{\mathcal{F}}{V}\right) \quad (44)$$

which leads to

$$\pi = C + \frac{bS^2C^2}{2} + \frac{cS^3C^3}{3} + \frac{E^2}{2\beta}\left(C\frac{\partial\epsilon}{\partial C} - \epsilon + \epsilon_s\right) \quad (45)$$

$$\mu = \mu_1 + \ln(C\nu_r) + bS^2C + \frac{cS^3C^2}{2} + \frac{E^2}{2\beta}\left(\frac{\partial\epsilon}{\partial C} - \epsilon_s\nu_r N\right) \quad (46)$$

where μ_1 is a constant. The critical point, at the maximum of the demixing curve, is given by the two conditions

$$\partial\mu/\partial C = 0 \quad (47)$$

$$\partial^2\mu/\partial C^2 = 0 \quad (48)$$

Explicitly, these equations give rise to two approximate equations for the new critical concentration $C_c(E)$ and the new critical two-body interaction parameter $b_c(E)$ when the field is on

$$\frac{E^2}{2\beta_c}\left(\frac{\partial^2\epsilon}{\partial C^2}\right)_c \cong -\frac{1}{C_c(E)} - b_c(E)\,S^2 - cS^3C_c(E) \quad (49)$$

$$\frac{E_2}{2\beta_c}\frac{\partial}{\partial C}\left(\frac{\partial^2\epsilon}{\partial C^2}\right)_c \cong \frac{1}{C_c(E)^2} - cS^3 \quad (50)$$

where the index c indicates the equilibrium critical value in the absence of a field. Solutions of eqs 49 and 50 are given to first order by

$$C_c(E) \cong C_c - C_c\frac{E^2}{4\beta_c}\left(\frac{\partial^3\epsilon}{\partial C^3}\right)_c \quad (51)$$

$$b_c(E) \cong b_c - \frac{E^2}{2\beta_c S^2}\left(\frac{\partial^2\epsilon}{\partial C^2}\right)_c \quad (52)$$

where

$$C_c = c^{-1/2}S^{-3/2} \quad (53)$$

$$b_c = -2S^{-1/2}c^{1/2} \quad (54)$$

Demixing occurs when $b < b_c(E)$. Since the refractive index of the solution is $n = \sqrt{\epsilon}$, then

$$\epsilon \cong \epsilon_s + \left(\frac{\partial\epsilon}{\partial C}\right)C + \frac{1}{2}\left(\frac{\partial^2\epsilon}{\partial C^2}\right)C^2 = \epsilon_s + 2n_s\left(\frac{\partial n}{\partial C}\right)C + \left(\frac{\partial n}{\partial C}\right)^2C^2 \quad (55)$$

where $(\partial n/\partial C)$ is assumed to be constant, for low polymer concentrations. Using this last equality, eqs 51 and 52 can be rearranged as follows:

$$\Delta C = C_c(E) - C_c \cong 0 \quad (56)$$

$$\Delta b = b_c(E) - b_c = -\frac{E^2}{\beta_c S^2}\left(\frac{\partial n}{\partial C}\right)^2 < 0 \quad (57)$$

The inequality eq 57 predicts that electric-field-induced remixing of a binary liquid mixture at a temperature just below the critical temperature is possible. Note that it is straightforward to show that these conclusions still hold for the case of a low-molecular-weight mixture with a simple lattice model as used by Debye and Kleboth.[6] Notice also that, more generally, eq 52 predicts that b_c is shifted if the curve of the dielectric constant as a function of the polymer concentration possesses a curvature. However, since $\partial n/\partial C$ can be assumed to be a constant for a semidilute polymer solution, the effect of an electric field is to decrease the critical two-body interaction parameter. For a polymer solution such as polystyrene/cyclohexane in the poor solvent region at its critical concentration (which depends on the molecular weight), the two-body interaction parameter is an inverse function of the temperature.[24] Thus, simple manipulations show that the change in the critical point due to the field scales as

$$\frac{T_c(E) - T_c}{T_c} \sim -E^2\left(\frac{\partial n}{\partial C}\right)^2 \quad (58)$$

Therefore, the effect of the electric field is to decrease the critical temperature; this effect is quadratic in the field strength and quadratic in the refractive index increment. Notice that the critical shift is independent of the molecular weight of the polymer. Thus, it is expected that electric-field-induced remixing is feasible for low-molecular-weight systems.

Below the critical temperature, the parametric equations of the coexistence curves with and without a field are obtained by use of Maxwell's rule for the continuous model:[24]

$$\mu(C^I) = \mu(C^{II}) \quad (59)$$

$$\int_{C^I}^{C^{II}} C\left(\frac{\partial\mu}{\partial C}\right)dC = 0 \quad (60)$$

where C^I and C^{II} are the polymer concentrations in the sol phase and in the gel phase. These two conditions imply the equality of both the chemical potential and the osmotic pressure in the two phases. The coexistence curve can be calculated by using eqs 59 and 60 and can be written in terms of the parameter $t = C^{II}/C^I$, the dimensionless polymer concentration $C' = C^IS^{3/2}c^{1/2}$ in the dilute phase, and the dimensionless two-body interaction parameter b'

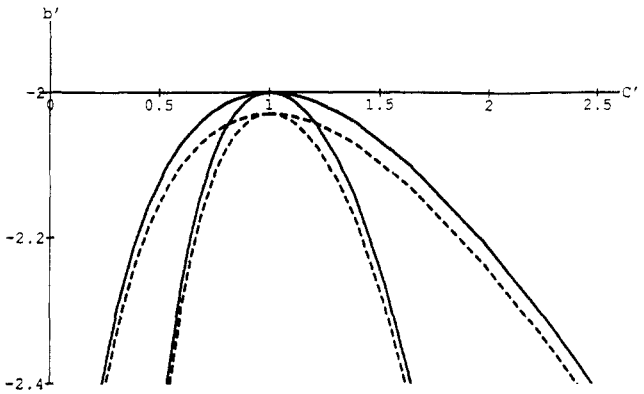

Figure 3. Coexistence curves and spinodal curves with (dashed lines) and without an electric field (solid lines). The effect of the field is to lower both the coexistence curve and the spinodal curve, allowing the effect of electric-field-induced remixing. The dimensionless electric field $\bar{E}$, defined in the text, is $\bar{E}^2 = 0.03$ in this case.

$= bS^{1/2}c^{-1/2}$.[24] The parametric equations of the coexistence curve, in the presence of an electric field, are

$$C_{co}'(t) = \frac{\sqrt{6(t+1)\ln t - 12(t-1)}}{(t-1)^{3/2}} \tag{61}$$

$$b_{co}'[t,C_{co}'(t)] = -\frac{2}{(t+1)C_{co}'(t)} - \frac{2C_{co}'(t)\,(t^2+t+1)}{3(t+1)} - \bar{E}^2 \tag{62}$$

where $\bar{E}^2 = (E^2/\beta S^{3/2}c^{1/2})(\partial n/\partial C)^2$ and $t \geq 1$. When $\bar{E} = 0$, the equilibrium parametric solutions given in ref 24 are recovered.

The spinodal curve, which corresponds to the inflection points of $\mathcal{F}/V$, is given by the equation

$$b_s' = -\frac{1}{C'} - C' - \bar{E}^2 \tag{63}$$

Figure 3 shows coexistence curves as well as spinodal curves in the presence and absence of an electric field. These curves display the same highly asymmetric profiles with the top of the demixing curve at $C' = 1$ and shifted to lower values of b' as stronger electric fields are applied. If a polymer/solvent system is at a constant temperature below the unperturbed coexistence curve and above the coexistence curve in the presence of an electric field, it can be remixed by means of an electric field (e.g., point P in Figure 4). Figure 4 also shows that electric field-induced remixing is facilitated for systems that have an overall polymer concentration larger than the critical concentration. It becomes more difficult to induce this effect for concentrations smaller than C_c since the coexistence curves in the presence and absence of an electric field merge for dilute polymer solutions.

The top of the demixing curve when the electric field is applied is given approximately by ($t \cong 1$):

$$\left(1 + \frac{\bar{E}^2}{2}\right)\left(\frac{b - b_c(E)}{b_c(E)}\right) \cong \frac{(t-1)^2}{24} \tag{64}$$

Since $t = C^{II}/C^{I}$, the last expression can be rewritten as follows:

$$\frac{C^{II} - C^{I}}{C^{I}} = (t-1) = \left[24\left(1 + \frac{\bar{E}^2}{2}\right)\left(\frac{b - b_c(E)}{b_c(E)}\right)\right]^{1/2} \tag{65}$$

This assesses one of the limits of the above mean-field

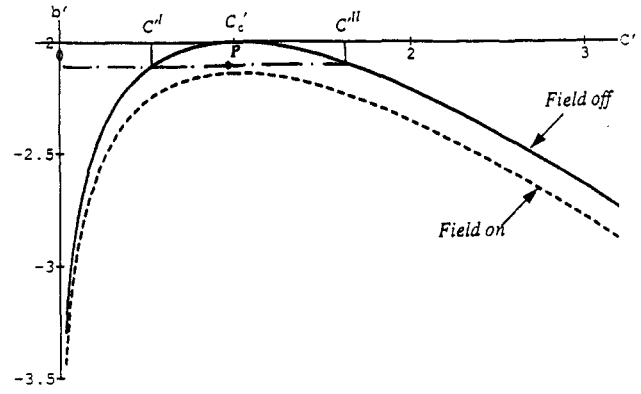

Figure 4. Coexistence curves with (dashed line) and without a field (solid line). This graph shows that a two-phase polymer/solvent system such as P below the coexistence curve without a field and above the new coexistence curve with a field ($\bar{E}^2 = 0.14$) can be remixed. This figure shows that electric-field-induced remixing of dilute solutions is more difficult than for semidilute solutions.

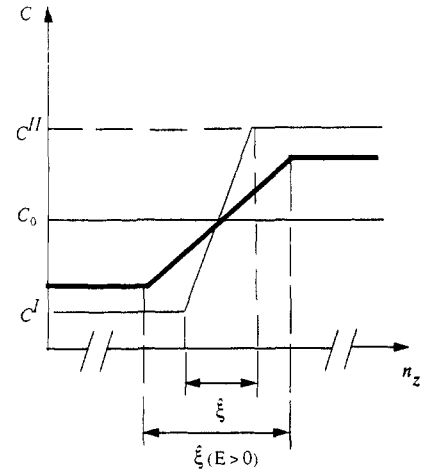

Figure 5. Schemes of the concentration profiles across the interface between the semidilute phase and the dilute phase with and without the field. The effect of an electric field is to increase the thickness of the interface facilitating induced remixing of the phase-separated solution. When a system such as P in Figure 4 is subject to a field, the thickness of the interface diverges.

approximation. More rigorous calculations in the framework of the renormalization group theory applied to critical phenomena show that in the absence of an external field $(C^{II} - C^{I})/C^{I} \sim ((b - b_c)/b_c)^{\beta}$ where $\beta \approx 1/3$ instead of $1/2$.[11] Note also that the influence of polymer polydispersity and molecular weight distribution on the location of the critical point has not been taken into consideration. Indeed longer chains precipitate before shorter chains which induces a shift of the critical point toward higher concentrations and lower temperatures. Therefore, the critical point is, in general, not at the top of the coexistence curve.

Below the critical temperature, the length scale over which the concentration profile decays from its maximum value, C^{II}, in the polymer-rich phase to its minimum value, C^{I}, in the dilute phase defines a new correlation length $\hat{\xi}$ (see Figure 5). $\hat{\xi}$ is the thickness of the interface between the two phases. If the concentration variation between the two phases is sharp, the kinetics of remixing is slow and vice versa. Scaling laws suggest the following form for $\hat{\xi}$:[20]

$$\hat{\xi} = a/NC^{II}\nu_r \tag{66}$$

where a is the parameter of the lattice of the Flory–Huggins model ($a = \nu_r^{1/3}$). Figure 5 shows that, at a constant

Table I
Critical Temperatures and Critical Polymer Volume Fractions

M_w (10^6)	T_c (°C)	φc	M_w/M_n
1.8	30.50	3.054	1.06
0.9	29.17	4.026	1.04
0.6	28.17	4.708	1.04
0.4	26.35	5.488	1.05

temperature, the effect of an electric field is to decrease the concentration of the semidilute phase and to increase the concentration of the dilute phase (see Figure 5). Therefore, the thickness of the interface increases, facilitating field-induced remixing. In that figure, $\mathbf{n}_z$ describes the direction of gravity. The rate at which a new one-phase equilibrium is reached depends on the field strength, the molecular weight of the polymer, the temperature, and the refractive index increment of the polymer solution. For systems under conditions as described by P in Figure 4, the thickness of the interface diverges; in other words, the system is in one phase.

As pointed out by Helfand and Fredickson,[15] this general thermodynamic approach is illegitimate when applied to the case of shear flow-induced "apparent" phase separation where one would add polymer conformational and entropic terms due to shear to the Flory–Huggins free energy of mixing. The main reason for this is that a polymer solution subject to shear flow is far from equilibrium, compared to the present case where, once steady state is reached, the system is in equilibrium. However, it is expected that such a thermodynamic approach could be used in a potential flow, e.g., an extensional flow as studied by van Egmond and Fuller.[26]

3. Materials and Experimental Methods

3.1. Polymer Solution. The polymer samples were polystyrene (PS) standards (molecular weight range from 400 000 to 1 800 000) purchased from Pressure Chemicals Co., Pittsburgh, PA. The samples were used without further purification and dissolved in spectrophotometric-grade cyclohexane (CH) to prepare PS/CH semidilute solutions at the critical concentrations for the different molecular weights given in Table I. The inverse of the critical temperature T_c and the critical polymer volume fraction φ_c for PS/CH solutions are linear functions of $P^{-1/3}$ and $P^{-1/2}$, respectively, where $P = (\nu p/V_0)M_w$. ν_p is the partial specific volume of the polymer (ν_p = 0.9343 cm^3/g) and V_0 is the molar volume of the solvent (V_0 = 108.76 cm^3/mol).[27] Using critical data from the literature,[27-30] values of T_c and φ_c were interpolated for the different PS samples.

3.2. Small-Angle Light Scattering. Small-angle light scattering (SALS) allows for the measurement of structure factors in the plane perpendicular to the incident light. As shown above, the different moments of the structure factor including birefringence and dichroism can be computed. The light scattering apparatus is adapted from ref 4. This setup is used to study the electric-field-induced structure of polymer solutions both above the coexistence curve and below where the solutions are phase-separated. The light from an 8-mW Uniphase He–Ne laser of wavelength 632.8 nm is incident upon a Kerr cell containing the scattering solution maintained at constant temperature by a Neslab thermal bath with an accuracy of 0.01 °C. The body of the cell is made of black delrin and parallel-plate stainless steel electrodes that are 1.65 mm apart and 9 mm high. Concentration fluctuations in the polymer solution scatter light at different scattering angles onto a screen placed perpendicular to the incident light, while the transmitted beam passes through a hole in the middle of the screen. Pictures of the time-dependent SALS patterns are recorded with a CCD array camera at a rate of up to 3 images/s.

3.3. Dichroism. Scattering dichroism from the semidilute polymer solutions is measured with a rheooptical setup.[31] The optical train consists of a He–Ne laser, a polarizer at 0°, a photoelastic modulator at 45° placed before the Kerr cell containing the polymer solution, and a photodiode as detector. The polarization of the light is modulated at a frequency of approximately 50 kHz and demodulated by phase lock-in amplifiers to determine scattering dichroism. Dichroism measurements probe the time-dependent field-induced anisotropy predicted by eq 33 relating dichroism to SALS structure factor measurements in the critical region above the quiescent coexistence curve. Moreover, measurements of the transmitted intensity (the dc signal from the detector) permit one to probe the influence of an electric field on the turbidity of the sample.

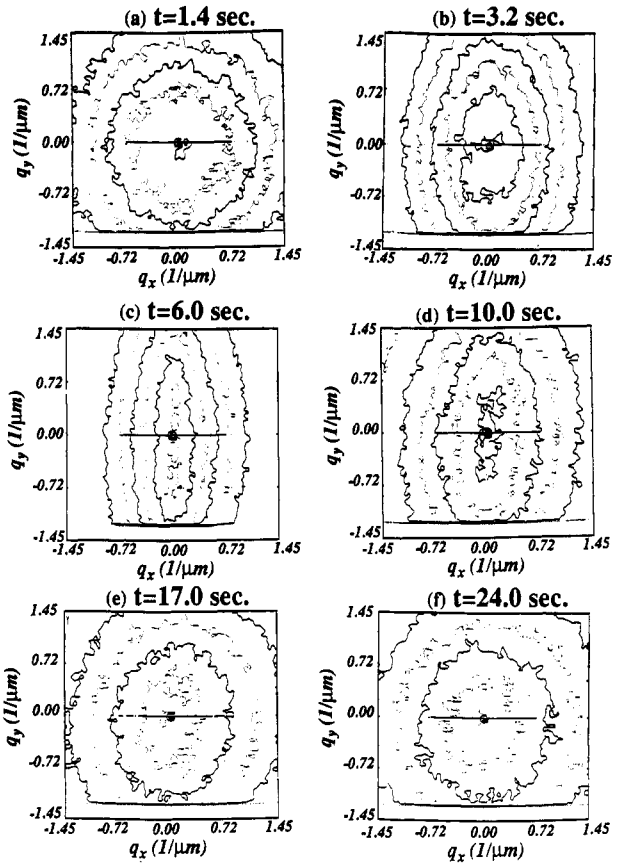

Figure 6. Contour plots of time-dependent scattering intensities. The electric field, applied from left to right, is turned on at t = 0.5 s and turned off at t = 6.5 s; $T - T_c$ = 0.03 °C, E = 5000 V/cm: (a) t = 1.4 s, (b) t = 3.2 s, (c) t = 6.0 s (steady state), (d) t = 10.0 s, (e) t = 17 s, (f) t = 24 s. The system investigated is a PS/CH solution (M_w = 600 000) at its critical concentration (φ = 4.7 vol %).

4. Results and Discussion

4.1. Time-Dependent Small-Angle Light Scattering. Figure 6 shows a set of SALS patterns for a typical experiment. The system investigated is a PS/CH solution (M_w = 600 000) at its critical concentration (φ = 4.71 vol %) above the critical temperature ($T - T_c$ = 0.03 °C). The different times at which the pictures were taken are indicated in the figure, and the electric field (5000 V/cm) is applied in the horizontal direction. Contour plots are lines of equal scattering intensity measured in the plane perpendicular to the incident light. As expected, in the absence of an electric field scattering patterns are concentric circles. Once a field is applied (t = 1.0 s), scattering patterns are deformed anisotropically and take on the shape of ellipses with the minor axis parallel to the field as predicted by eq 30. Upon cessation of the field (t = 6.5 s), scattering patterns relax to their initial isotropic form.

It is notable that the development of the elliptical patterns is caused only by compression of the isointensity contours along the field direction and is not accompanied

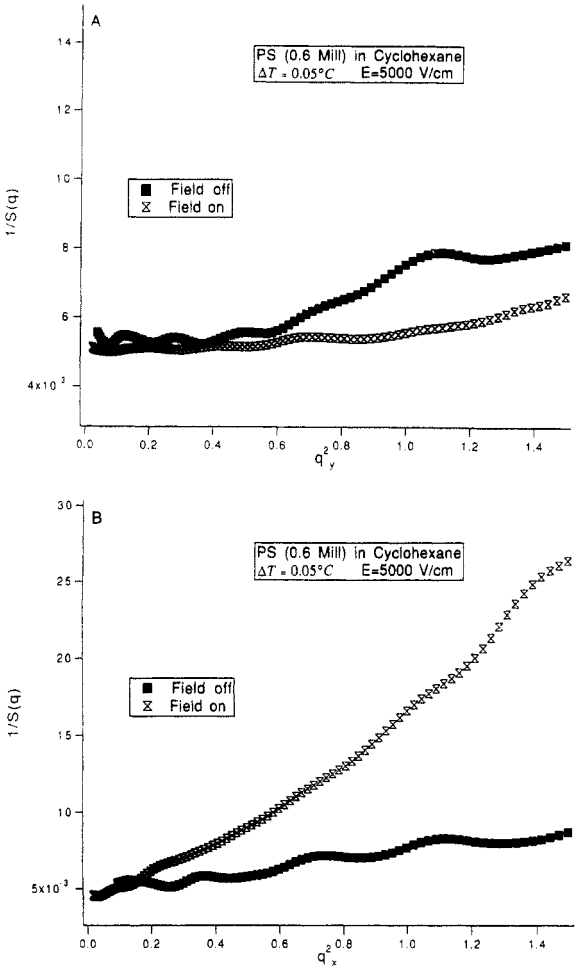

Figure 7. (A) Inverse of the structure factor versus the square of the scattering vector in the direction perpendicular to the electric field. The ratio of the slope to the intercept is the "transverse" correlation length which is decreased from ξ to ξ_E. PS/CH solution (M_w = 600 000) at its critical concentration (φ = 4.7 vol %) above the critical temperature ($T - T_c$ = 0.05 °C). E = 5000 V/cm. (B) Inverse of the structure factor versus the square of the scattering vector in the direction of the electric field. The longitudinal correlation length is modified from ξ to $\xi_E[1 + (K_3/K_1)E^2]^{0.5}$. Same conditions as in Figure 7A.

by an elongation along the perpendicular direction. This effect is demonstrated in parts A and B of Figure 7 where the inverse of the scattering intensity is plotted versus the square of the scattering vector along the major and minor axes (PS/CH solution, M_w = 600 000, $T - T_c$ = 0.05 °C). In the absence of any field, such plots show straight lines as expected from the form of the Orstein–Zernike structure factor. In particular, Figure 7A shows that the effect of the electric field is small in the direction perpendicular to the field, which confirms the predictions of the above mean-field theory. ξ_E can be computed from the same figure, because the ratio of the slope to the intercept is equal to the square of the equilibrium correlation length. When the field is applied, the transverse correlation length (the average size of the concentration fluctuations perpendicular to the direction of the field) is diminished from $\xi \sim (T - T_c)^{-0.5}$ to $\xi_E \sim [T - T_c(E)]^{-0.5}$. A ratio $\xi_E/\xi \cong 0.7$ was obtained for a critical PS/CH (M_w = 600 000) submitted to a 5000 V/cm steady electric field at a temperature $T - T_c$ = 0.05 °C. This corresponds to a shift in the critical temperature of about $T_c - T_c(E) \cong 0.04$ °C. To check this rough estimate of $T_c(E)$, several "electric-field-induced remixing" experiments were conducted with the same polymer solution at different temperatures T such that $T_c \leq T \leq T_c(E)$. It was found that, indeed, remixing was possible only for temperatures as low as $T_c - T = T_c - T_c(E) \cong 0.05$ °C for the same field strength. Further explanations are given in section 4.3. The same procedure could be performed at different polymer concentrations for a constant field strength; therefore, the new coexistence curve (with the field) can be plotted point by point. On the other hand, Figure 7B shows a dramatic increase in the slope of the line along the minor axis of the ellipses when the field is applied. If a longitudinal correlation length of the critical fluctuations is defined in the direction of the field, then the effect of an electric field is to increase the longitudinal correlation length quadratically with the field strength.

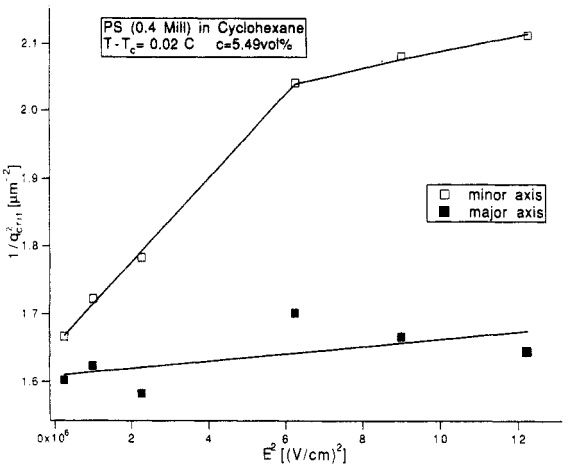

Figure 8. Inverse of the square of the length of both the minor axis and the major axis of the elliptical scattering patterns as a function of the square of the electric field. Only the length of the minor axis is decreased as an electric field is applied. PS/CH solution (M_w = 400 000) at its critical concentration (φ = 5.49 vol %) above the critical temperature ($T - T_c$ = 0.02 °C). E = 5000 V/cm.

Figure 8 shows the square of the inverse of the length of the minor axis and the major axis, respectively, versus E^2 for a PS/CH solution (M_w = 400 000) at constant temperature ($T - T_c$ = 0.02 °C). Both lengths are computed with eq 31 using SALS measurements. As predicted by the above mean-field theory, only the inverse of the length of the minor axis increases remarkably with growing field strength. In contrast, the length of the major axis remains approximately constant within the experimental range of electric field strengths. Such a plot can be used to measure the two-body parameter K_3 by computing the slope of the line. A more detailed discussion of the influence of the temperature and the concentration on K_3 will be presented in a future paper.

4.2. Scattering Dichroism. In view of Onuki and Doi's predictions,[22] one expects both birefringence and form dichroism to be enhanced as the concentration fluctuations become of the magnitude of the wavelength of the incident light. If dichroism, defined as the difference of the principal values of the imaginary component of the refractive index tensor n, is caused by anisotropic scattering from the concentration fluctuations (form dichroism), then it should be positive. Calibration of the experiment with a polarizer that has by definition infinite negative dichroism allows us to determine the sign of the dichroism. Dichroism measurements were verified to be positive in the critical region up to about 0.15 °C above the coexistence curve for all the critical PS/CH solutions.

Figure 9 shows a typical example of measured electric dichroism for a sample of PS/CH (M_w = 600 000, φ = 2.6 vol %) at $T - T_c$ = 0.05 °C. The electric field is applied at the time indicated by the arrow, and anisotropic

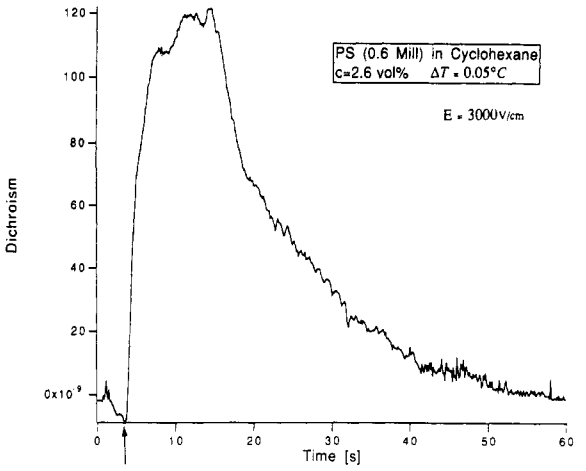

Figure 9. Time-dependent electric-field-induced scattering dichroism as measured by an optical rheometer. PS/CH solution (M_w = 600 000) at $T - T_c$ = 0.05 °C, φ = 2.6 vol %. The electric field is applied at the time indicated by the arrow. E = 3000 V/cm.

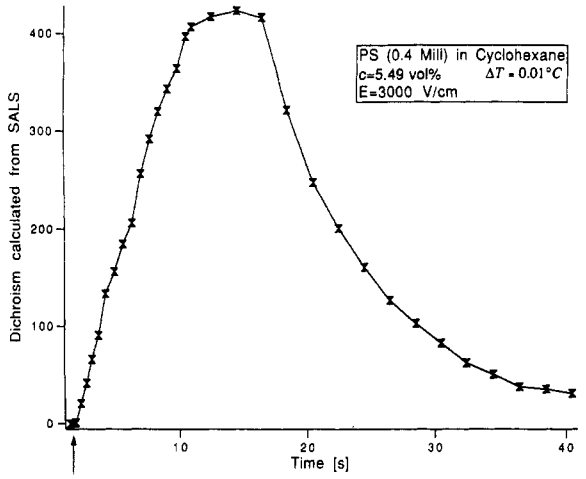

Figure 10. Time-dependent electric-field-induced scattering dichroism, calculated from SALS measurements using eq 33. PS/CH solution (M_w = 400 000) at $T - T_c$ = 0.01 °C, φ = 5.49 vol %. The electric field is applied at the time indicated by the arrow. E = 3000 V/cm.

deformation of the concentration fluctuations leads to scattering dichroism, which increases until a steady-state value is reached. Once the field is turned off, concentration fluctuations relax by diffusion. To our knowledge, this is the first time that electric-field-induced enhanced dichroism in a critical polymer solution has been observed. As expected, in the critical region the rise time is shorter than the relaxation time for a large range of field strengths. In addition, time-dependent SALS and scattering dichroism measurements have shown that relaxation times increase dramatically as the quiescent phase-separation point is approached, which is an illustration of the well-known critical "slowing down" effect. Scattering dichroism computed from eq 33 using measured values of the SALS structure factors is displayed in Figure 10 for a PS/CH solution (M_w = 400 000, φ = 5.49 vol % at $T - T_c$ = 0.01 °C). Measured steady-state values of dichroism are in fairly good agreement with calculated values of dichroism as in the case of shear flow-induced fluctuation enhancement.[4] Figure 11 shows a series of dichroism measurements at different electric field strengths for a PS/CH solution (M_w = 400 000, φ = 5.49 vol %, $T - T_c$ = 0.10 °C). The rise time upon inception of the orienting field is observed to decrease with increasing field strength, while relaxation times are independent of the field strength as

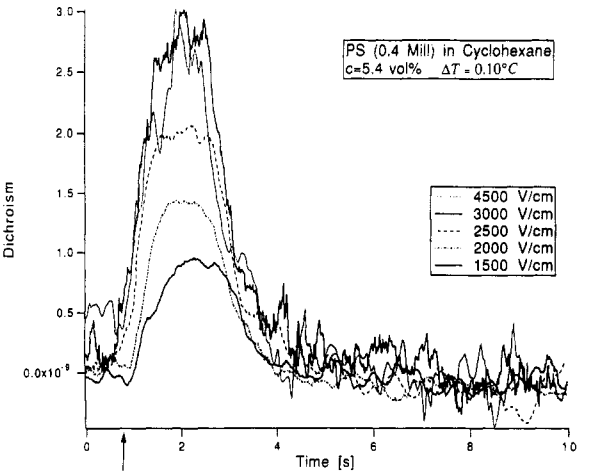

Figure 11. Time-dependent measurements of scattering dichroism at electric fields ranging from 1500 to 4500 V/cm. The effect of the field is to decrease the rise time to reach steady state and to increase quadratically the steady-state dichroism before reaching saturation. PS/CH solution (M_w = 400 000) at $T - T_c$ = 0.10 °C, φ = 5.40 vol %. The electric field is applied at the time indicated by the arrow.

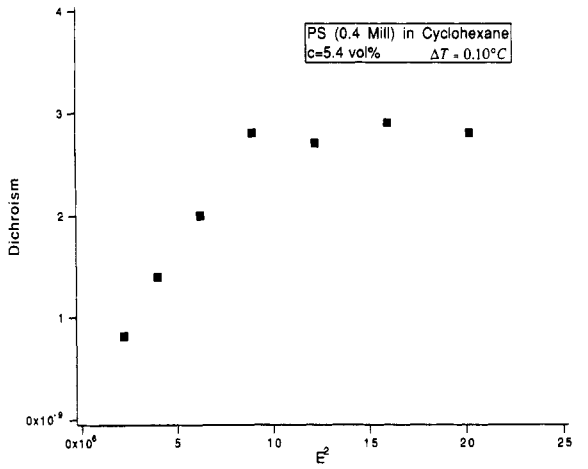

Figure 12. Steady-state values of scattering dichroism as a function of E^2. Same conditions as in Figure 11.

expected. In Figure 12, it is verified that scattering dichroism follows a quadratic law in the field strength at low fields (M_w = 400 000, φ = 5.49 vol % at $T - T_c$ = 0.1 °C). At large field strengths, steady-state scattering dichroism reaches a plateau. It was observed that the field strength at which saturation occurred decreased with the molecular weight of the polymer.

Figure 2 predicts the existence of a temperature, T_m, at which induced anisotropy is maximum. Below and above T_m, scattering dichroism diminishes sharply. Figure 13 confirms qualitatively these predictions for a PS/CH solution (M_w = 600 000, φ = 2.6 vol %). Steady-state scattering dichroism is plotted vs $T - T_c$ for a constant value of field strength. It substantiates the existence of a narrow temperature range where form dichroism is greatly enhanced. In both the hydrodynamic region ($T - T_c \gg 0.05$ °C) and the "extreme" critical region ($T - T_c \ll 0.05$ °C) scattering decreases an order of magnitude within $|T - T_m| \cong 0.04$ °C. The existence of T_m below and above which scattering dichroism diminishes can be explained physically. Indeed, as the temperature distance from the quiescent coexistence curve is decreased, the size of the concentration fluctuations increases and eventually the wavelength of the incident light becomes larger than the correlation length of the fluctuations. This causes the electric-field-induced anisotropy to become "transparent"

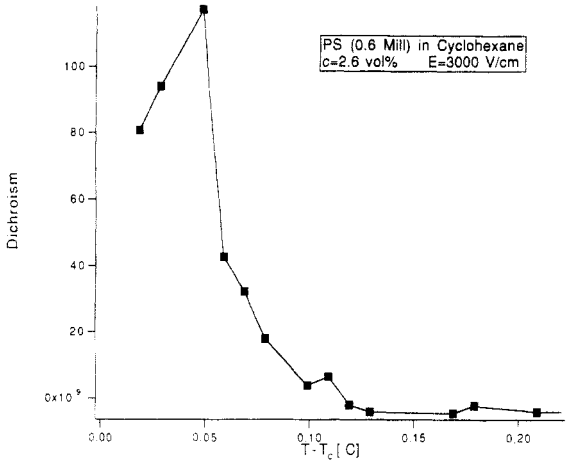

Figure 13. Steady-state values of scattering dichroism as a function of $T - T_c$. PS/CH solution (M_w = 600 000), φ = 2.6 vol %. E = 3000 V/cm.

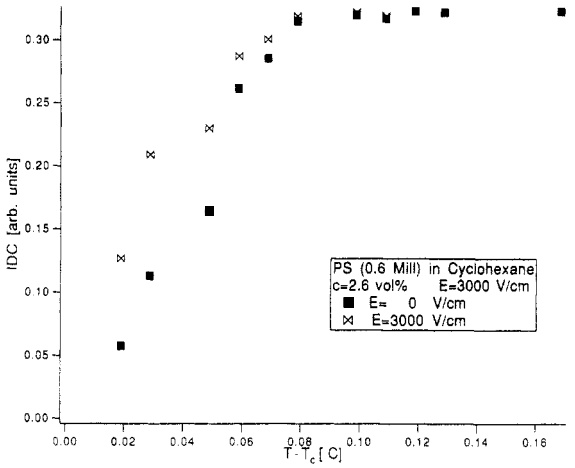

Figure 14. Transmitted intensity as a function of $T - T_c$ for a PS/CH solution (M_w = 600 000) with (open symbols) and without (filled symbols) an electric field, φ = 2.6 vol %, E = 3000 V/cm.

to the probing light. Conversely, when the temperature of the polymer solution is increased, above T_m, the size of the fluctuations diminishes as $(T - T_c)^{-0.5}$, causing scattering dichroism to decrease dramatically. Eventually, far away from the critical point, concentration fluctuations become too small to give rise to any measurable optical anisotropy.

As mentioned earlier, another effect of an applied electric field on a binary mixture is to increase the transmitted intensity, meaning to decrease the turbidity. This effect was observed for the first time by Debye and Kleboth[6] for a critical low-molecular-weight solution above T_c. It is examined in Figure 14, where transmitted intensities with and without applied field are plotted as a function of $T - T_c$ for a PS/CH solution (M_w = 600 000, φ = 2.6 vol %). The quiescent turbidity increases as the size of the concentration fluctuations grows ($T \rightarrow T_c$) and becomes of the same order as the wavelength of the probing light ($\xi \sim 1/\lambda_i$). As an electric field (E = 3000 V/cm) is applied to the polymer solution, the turbidity decreases substantially; this effect becomes stronger as the critical point is approached. In the hydrodynamic region ($T - T_c \sim 0.09$ °C), this critical effect becomes too weak to be measurable. The top curve in Figure 15 shows that this electric-field-induced enhancement of the transmitted intensity is accompanied by a decrease of the total scattering intensity for temperatures above the quiescent coexistence curve. The electric-field-induced decrease of the turbidity can be partially explained by a shift in the critical temperature

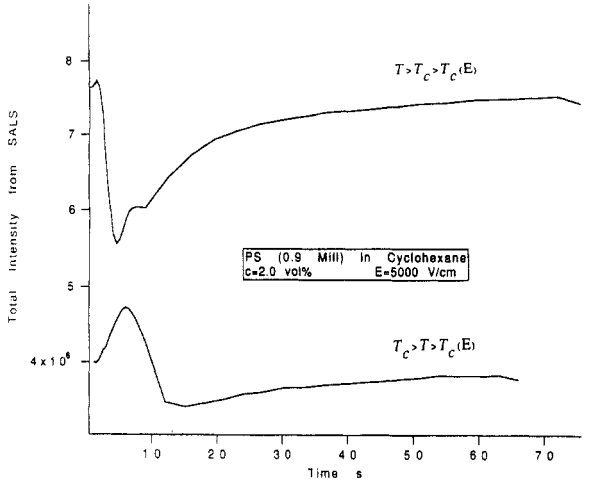

Figure 15. Time-dependent total scattering intensities below and above the critical point. PS/CH solution (M_w = 900 000), φ = 2.0 vol %, E = 5000 V/cm. When steady state is reached, the electric field is turned off.

as predicted by eq 33. However, it is interesting to notice that an additional term $|\nabla \times \mathbf{E}\delta c|^2$ in eq 8 would contribute to enhanced forward scattering as well

$$\frac{1}{2}C_5\int d\mathbf{r}\,|\nabla \times \mathbf{E}\delta c|^2 = \frac{1}{2}\sum_{\mathbf{q}} C_5 E^2(q_z^2 + q_y^2)|\delta c(\mathbf{q})|^2 \quad (67)$$

However, C_5 must be smaller than C_4 since the second term in eq 67 would simultaneously diminish anisotropy in the $q_x - q_y$ plane. More explanations for Figure 15 are given in section 4.3.

Measurements of relaxation times as a function of $T - T_c$ and M_w will be presented in another paper.

4.3. Electric-Field-Induced Remixing. A polymer solution with an overall concentration close to the critical concentration demixes macroscopically into a semidilute phase and a dilute phase below its coexistence curve. In section 2.3, it is shown that an applied electric field not only decreases the critical value of the two-body parameter b from b_c to $b_c(E)$ but also lowers both the coexistence curve and the spinodal curve. The effect is quadratic in the electric field. The SALS technique allows one to observe that electric fields ranging from 500 to 10 000 V/cm induce remixing of the two phases at temperatures sufficiently close to the coexistence curve in a period of time that increases with molecular weights that ranged from 400 000 to 1 800 000 and decrease with the field strength. While the solution is remixing, the scattering intensity increases and displays the usual elliptical patterns in the plane perpendicular to the incident light. When the applied field is turned off, the solution becomes turbid in a few seconds. Figure 16 shows a typical set of SALS images of a field-induced remixing experiment at $T - T_c$ = −0.04 °C; the sample molecular weight is M_w = 600 000 and its volume fraction is $\varphi = \varphi_c$ = 4.708. Times at which frames were taken are indicated on the figure. Numbers along the isointensity contours are expressed in arbitrary units. In the first frame, the scattering intensity is very low since the turbidity is high. In the following frames, when the field is applied (t = 1.5 s), one can observe a dramatic increase of the scattering intensity and at the same time formation of elliptical patterns. The polymer/solvent system ultimately behaves like a solution above the coexistence curve. This is an indication of the phenomenon of electric-field-induced remixing as predicted by the mean-field theory. When the field is turned off (t = 7.5 s), the elliptical patterns relax toward circular patterns while the increasing turbidity due to demixing

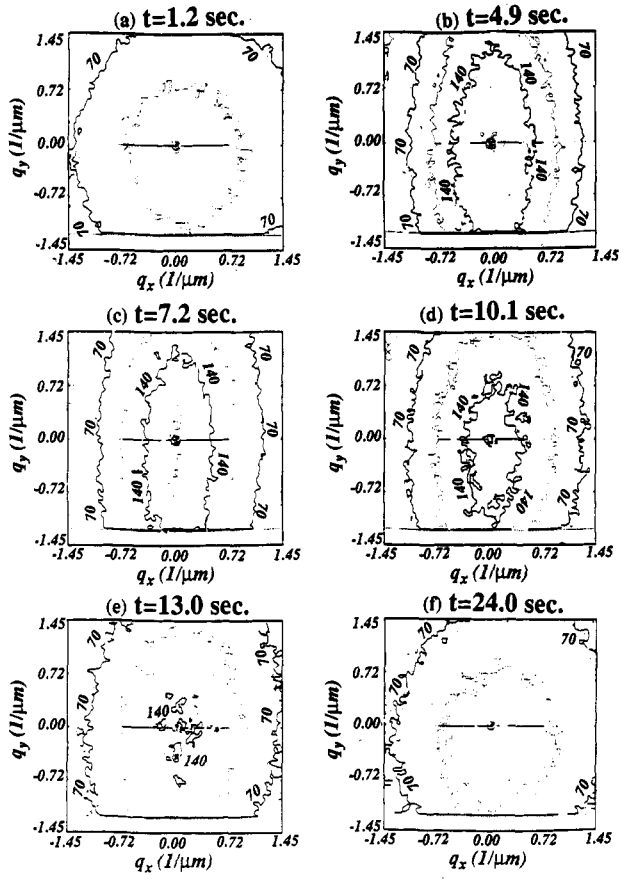

Figure 16. Contour plots of time-dependent scattering intensities for an "electric-field-induced" experiment. The electric field, applied from both left to right, is turned on at t = 0.5 s and turned off at t = 10 s; $T_c - T$ = 0.03 °C, E = 5000 V/cm: (a) t = 1.2 s, (b) t = 4.9 s, (c) t = 7.2 s (steady state), (d) t = 10.1 s, (e) t = 13 s, (f) t = 24 s. PS/CH solution (M_w = 600 000) at its critical concentration (φ = 4.7 vol %).

reduces the scattering intensity. Electric-field-induced remixing is also demonstrated with the lower curve in Figure 15, where it is seen that the effect of the electric field is to increase dramatically the total scattering intensity for a PS/CH solution at a temperature below the quiescent coexistence curve.

Experiments conducted at temperatures $T < T_c(E)$ show that remixing is not possible for a given value of the applied field at an overall concentration close to C_c as predicted by the conditions in eq 57. On the other hand, dilute solutions ($C \ll C_c$) of PS/CH below their cloud point cannot be remixed as predicted above in Figure 4.

Note that according to eq 58 electric-field-induced remixing is possible for lower-molecular-weight solutions. This prediction is checked by observing electric-field-induced remixing for a low-molecular-weight critical solution of nitrobenzene/*n*-hexane. Remixing does indeed occur, but the time scales are much shorter than for the polystyrene solutions: the remixing occurs at about 0.05 °C below the cloud point for the same field strength. However, a detailed study of the kinetics of remixing still remains to be done both experimentally and theoretically.

In section 4.1, it is shown that plots of the inverse of the structure factor versus q_y^2 can determine the transverse correlation length $\xi_E = \xi_0[(T - T_c(E))/T_c]^{-\nu}$ and, therefore, $T_c(E)$. Figure 15 presents another method to determine the coexistence curve in the presence of an electric field for a given field strength. The total scattered intensity is measured using SALS for a PS/CH solution (M_w = 900 000). As the temperature of the polymer/solvent system is lowered, above the cloud point ($T > T_c > T_c(E)$), corresponding to the top curve in Figure 15, the total intensity decreases when the field is applied and increases as the field is turned off due to the shift of the coexistence curve. Whereas for a system represented by the point P in Figure 4 ($T_c > T \geq T_c(E)$), corresponding to the lower curve in Figure 15, the intensity increases when the field was turned on and decreases when the field is turned off, which is indicative of electric-field-induced remixing. $T_c(E)$ is determined as soon as electric-field-induced remixing has become impossible.

5. Conclusions

In this paper we have studied electric-field-induced anisotropy and structure above and just below the quiescent coexistence curve of semidilute polymer solutions. Two new phenomena have been observed: enhanced electric dichroism in the one-phase region and electric-field-induced remixing in the two-phase region. Both phenomena can be qualitatively explained within the frame of a mean-field theory. In particular, it was shown that scattering dichroism was enhanced only in a narrow intermediate temperature region, between the critical region and the hydrodynamic region.

The effect of shear flow is to suppress concentration fluctuations in low-molecular-weight binary fluid mixtures, whereas fluctuations are enhanced in polymer/solvent systems, especially close to the coexistence curve; however, no phase transition occurs. In contrast, an electric field first acts on the equilibrium thermodynamics, inducing a shift of the critical temperature, and second it facilitates mechanisms of growth of the concentration waves in the direction of the field through dipolar interactions of the gradients of the fluctuations. More theoretical and experimental research is needed for this new problem. In particular, it is important to comprehend the pair interaction parameters K_2 and K_3 in the expression of the total free energy (eq 18) for a critical polymer/solvent system subject to an electric field, by deriving a molecular model. Another point of interest is why the corresponding electric interactions between concentration fluctuations and their gradients dominate dipole–dipole interactions that would instead deform circular patterns into "butterfly" patterns.[22] There might exist a crossover temperature below which butterfly patterns appear inside elliptical patterns at low scattering angles, as observed very recently for a polystyrene/poly(vinyl methyl ether) blend subject to low strain rates.[32] Saturation of the steady-state dichroism at large electric field strengths has to be further investigated as well. Moreover, a more accurate temperature control is necessary to compute the equilibrium coexistence curve in the presence of an applied field. This paper has emphasized equilibrium static structure measurements obtained for polymer/solvent systems near the coexistence curve; dynamics of the transitions are now being investigated using both time-dependent SALS and scattering dichroism.

Additionally, we observed that electric fields induced complex dynamics in physical gels obtained by precipitation of PS from critical PS/CH solutions below the coexistence curve. Elliptical patterns were observed to orient in the direction parallel to the uniaxial field. Then, these scattering patterns were transformed via an intermediate circular form to elliptical patterns with the major axis perpendicular to the direction of the applied field. This phenomenon is currently being studied using SALS.

Acknowledgment. This research has been partially supported by the NSF–MRL Center for Materials Re-

search at Stanford University. We acknowledge the cooperation of Jan van Egmond and Douglas Werner for setting up the SALS experiment and for rewarding discussions. K.B. thanks the Studienstiftung des Deutschen Volkes for financial support. We also thank M. Doi and A. Onuki for communicating ref 22 prior to its publication.

References and Notes

(1) Flory, P. J. In *Selected Works of Paul J. Flory*; Mandelkern, L., Mark, J. E., Suter, U. W., Yoon, D. Y., Eds.; Stanford University Press: Stanford, CA, 1985; Vol. I.
(2) Debye, P. *J. Chem. Phys.* **1962**, *36*, 851.
(3) Goulon, J.; Greffe, J.-L.; Oxtoby, D. W. *J. Chem. Phys.* **1979**, *70*, 4741.
(4) van Egmond, J. W.; Werner, D. E.; Fuller, G. G. *J. Chem. Phys.* **1992**, *96*, 7742.
(5) Onuki, A.; Oppenheim, I. *Phys. Rev. A* **1981**, *24*, 1520.
(6) Debye, P.; Kleboth, K. *J. Chem. Phys.* **1965**, *42*, 3155.
(7) Pyzuk, W. *Chem. Phys.* **1980**, *50*, 281.
(8) Degiorgio, V.; Piazza, R. *Phys. Rev. Lett.* **1985**, *55*, 288.
(9) (a) Bellini, T.; Degiorgio, V. *Phys. Rev. B* **1989**, *39*, 7263. (b) Degiorgio, V.; Bellini, T.; Piazza, R.; Mantegazza, F.; Goldstein, R. E. *Phys. Rev. Lett.* **1990**, *64*, 1043.
(10) Berne, B. J.; Pecora, R. *Dynamic Light Scattering*; Wiley: New York, 1976.
(11) Le Guillou, J. C.; Zinn-Justin, J. *Phys. Rev. Lett.* **1977**, *39*, 95.
(12) Goedel, W. A.; Zielesny, A.; Belkoura, L.; Engels, T.; Woermann, D. *Ber. Bunsen-Ges. Phys. Chem.* **1990**, *94*, 17.
(13) Landau, L. D.; Lifshitz, E. M. *Statistical Physics*; Pergamon Press: London, 1969.
(14) Jannink, G.; de Gennes, P.-G. *J. Chem. Phys.* **1968**, *48*, 2260.
(15) Helfand, E.; Fredrickson, G. H. *Phys. Rev. Lett.* **1989**, *62*, 2468.
(16) Milner, S. T. *Phys. Rev. Lett.* **1991**, *66*, 1477.
(17) Doi, M. In *Dynamics and Patterns in Complex Fluids*; Onuki, A., Kawasaki, K., Eds.; Springer Proceedings in Physics 52; Springer-Verlag: Heidelberg, Germany, 1990.
(18) Onuki, A. *J. Phys. Soc. Jpn.* **1990**, *59*, 3423.
(19) Doi, M.; Edwards, S. F. *The Theory of Polymer Dynamics*; Oxford University Press: Oxford, 1986.
(20) de Gennes, P.-G. *Scaling Concepts in Polymer Physics*; Cornell University Press: Ithaca, NY, 1980.
(21) Aharony, A. In *Phase Transitions and Critical Phenomena*; Domb, C., Green, M. S., Eds.; Academic Press: New York, 1976; Vol. 6.
(22) Onuki, A.; Doi, M. *Europhys. Lett.* **1992**, *17*, 63.
(23) Onuki, A.; Doi, M. *J. Chem. Phys.* **1986**, *85*, 1190.
(24) Des Cloizeaux, J.; Jannink, G. *Polymers in Solution*; Oxford University Press: Oxford, 1987.
(25) Jackson, J. D. *Classical Electrodynamics*, 2nd ed.; Wiley: New York, 1975.
(26) van Egmond, J. W.; Fuller, G. G. "Concentration Fluctuation Enhancement in Polymer Solutions by Extensional Flow", submitted to *Macromolecules*.
(27) Einaga, Y.; Ohashi, S.; Tong, Z.; Fujita, H. *Macromolecules* **1984**, *17*, 527.
(28) Karaya, N.; Unakite, M.; Kaneko, M. *Polymer* **1973**, *14*, 415.
(29) Nakata, M.; Dobashi, T.; Kuwahara, N.; Kaneko, M. *Phys. Rev. A* **1978**, *18*, 2683.
(30) Koningsveld, R.; Kleintjes, L. A.; Shultz, A. R. *J. Polym. Sci., Polym. Phys. Ed.* **1970**, *8*, 1261.
(31) Fuller, G. G.; Mikkelsen, K. J. *J. Rheol.* **1989**, *33*, 761.
(32) (a) Werner, D. E.; Fuller, G. G., in preparation. (b) Rabin, Y.; Bruinsma, R., preprint, 1992.

Registry No. PS, 9003-53-6; cyclohexane, 110-82-7.